

Supporting Information

Room-temperature processed ZrO₂ interlayer towards efficient planar perovskite solar cells

Jiawen Sun^{a,#}, Yuzhu Li^{a,#}, Naiwei Tang^a, Yang Zhou^a, Xiang Zhang^a, Xubing Lu^{a,*}, Xingsen Gao^a, Jinwei Gao^a, Lingling Shui^b, Sujuan Wu^{a,*}, Jun-Ming Liu^{a,c}

^a *Institute for Advanced Materials, South China Academy of Advanced Optoelectronics, South China Normal University, Guangzhou 510006, P. R. China.*

^b *Guangdong Provincial Key Laboratory of Optical Information Materials and Technology, South China Normal University, Guangzhou 510006, P. R. China.*

^c *Laboratory of Solid State Microstructures, Nanjing University, Nanjing 210093, P.R. China.*

*Corresponding Authors: sujwu@scnu.edu.cn, luxubing@m.scnu.edu.cn

#They contribute equally to this work.

Experimental section

Devices in this work were prepared and characterized by the materials and methods reported in our previous work.¹⁻² For ZrO₂ film, zirconium acetylacetone (Zr(AC)₄: 98%, Aladdin) were dissolved in DMF and stirred at 90 °C for 32 h to prepare precursor solution. After treating the ITO substrate by oxygen UV for 10 min, the precursor solution with various concentrations were spin-coated on the ITO

substrates at 500 rpm for 5 s and 5000 rpm for 40 s. Then ZrO₂ films were obtained by UV irradiation them for 45 min or annealing at 160 °C for 60 min.³⁻⁵ For the time-resolved photoluminescence (TRPL) spectra, it was recorded by a fluorescence spectrophotometer (Fluorolog-3, Horiba) and excited by a 473 nm pulse laser with the excitation energy of 100 mW and a rate of 5 MHz.

Table S1. Photovoltaic parameters of UV-PSCs with various zirconium precursor solution concentrations.

Concentration (mg/ml)	V _{oc} (V)	J _{sc} (mA/cm ²) ^c	J _{sc} (mA/cm ²) ^d	FF	PCE(%)
0	0.985	20.35	19.78	0.759	15.56 ^a (14.77) ^b
0.1	0.978	22.43	21.64	0.768	16.84 ^a (16.65) ^b
0.3	1.034	23.02	22.92	0.776	18.47 ^a (18.35) ^b
0.5	1.068	23.32	23.14	0.782	19.48 ^a (19.01) ^b
0.7	1.025	22.95	22.13	0.771	18.14 ^a (17.34) ^b

^a Champion efficiency. ^b Average PCE for 40 PSCs. ^c Measured J_{sc}. ^d Integrated current density from EQE.

Table S2. Photovoltaic parameters of UV-PSCs with different UV treatment time.

UV treatment time(min)	V _{oc} (V)	J _{sc} (mA/cm ²) ^c	J _{sc} (mA/cm ²) ^d	FF	PCE(%)
15	1.013	22.74	22.46	0.768	17.74 ^a (17.53) ^b
30	1.037	22.85	22.65	0.778	18.45 ^a (18.12) ^b
45	1.068	23.32	23.14	0.782	19.48 ^a (19.01) ^b
60	1.042	22.91	22.82	0.779	18.63 ^a (18.32) ^b
75	1.031	22.82	22.18	0.772	18.21 ^a (18.15) ^b

^a Champion efficiency. ^b Average PCE for 40 PSCs. ^c Measured J_{sc}. ^d Integrated current density from EQE.

Table S3. Photovoltaic parameters of Annealing-PSCs with different zirconium acetylacetone precursor solution concentrations.

Concentration (mg/ml)	V _{oc} (V)	J _{sc} (mA/cm ²) ^c	J _{sc} (mA/cm ²) ^d	FF	PCE(%)
0	0.985	20.35	19.78	0.759	15.56 ^a (14.77) ^b
0.1	0.988	21.24	21.04	0.769	16.67 ^a (16.48) ^b
0.3	0.997	23.02	22.94	0.772	17.73 ^a (17.25) ^b
0.5	1.042	23.28	23.26	0.781	18.51 ^a (17.63) ^b
0.7	0.991	23.01	22.43	0.768	17.52 ^a (17.21) ^b

^a Champion efficiency. ^b Average PCE for 40 PSCs. ^c Measured J_{sc}. ^d Integrated current density from EQE.

Table S4. Photovoltaic parameters of Annealing-PSCs with different annealing time.

Annealing Time (min)	V _{oc} (V)	J _{sc} (mA/cm ²) ^c	J _{sc} (mA/cm ²) ^d	FF	PCE(%)
15	0.973	21.61	21.46	0.754	15.86 ^a (15.57) ^b
30	0.986	22.52	22.43	0.764	16.97 ^a (16.45) ^b
45	1.013	23.11	22.95	0.773	17.83 ^a (17.49) ^b
60	1.042	23.28	23.26	0.781	18.51 ^a (17.63) ^b
75	0.995	23.06	22.89	0.769	17.65 ^a (17.39) ^b

^a

Champion efficiency. ^b Average PCE for 40 PSCs. ^c Measured J_{sc}. ^d Integrated current density from EQE.

Table S5 The values of R_{sh} , R_s and R_{sh}/R_s extracted from the J-V measurement of Reference-PSCs from 40 devices.

Reference-PSCs							
	R_s	R_{sh}	R_{sh}/R_s		R_s	R_{sh}	R_{sh}/R_s
1	111	15692	141	21	180	20339	113
2	154	26719	173	22	126	20357	161
3	121	23410	194	23	195	33727	173
4	122	22520	185	24	141	27413	195
5	138	28070	203	25	169	21595	128
6	137	34418	251	26	131	17788	136
7	104	19944	192	27	139	19932	143
8	135	27417	203	28	124	15507	125
9	115	24513	213	29	167	14397	86
10	138	32530	236	30	100	12602	126
11	112	10662	95	31	103	12591	122
12	117	24876	213	32	110	13744	125
13	106	14365	136	33	149	18808	126
14	127	18228	143	34	125	14357	115
15	135	16841	125	35	144	30684	213
16	100	13502	135	36	124	11927	96
17	160	20121	126	37	200	20634	103
18	160	19580	122	38	130	16287	125
16	114	14192	125	39	234	31549	135
20	103	12954	126	40	124	15507	125
Average		$R_s : 136$		$R_{sh} : 20258$		$R_{sh}/R_s : 150.2$	

Table S6 The values of R_{sh} , R_s and R_{sh}/R_s extracted from the J-V measurement of UV-PSCs from 40 devices.

UV-PSCs							
	R_s	R_{sh}	R_{sh}/R_s		R_s	R_{sh}	R_{sh}/R_s
1	106	40610	382	21	102	30787	301
2	94	30378	323	22	112	34909	311
3	97	33457	344	23	125	40293	323
4	112	37470	335	24	81	27954	345
5	105	37176	353	25	89	32286	363
6	116	46581	401	26	103	39031	378
7	94	32165	342	27	105	30857	293
8	97	34357	353	28	94	34615	367
9	103	37508	363	29	102	34009	334
10	72	27885	386	30	98	36549	372
11	96	42911	445	31	86	31740	368
12	102	36936	363	32	103	34473	336
13	104	38016	367	33	96	32939	342
14	101	35256	349	34	127	38161	301
15	94	32447	345	35	82	29947	363
16	101	39063	386	36	103	37898	368
17	99	36253	365	37	102	34376	336
18	75	31064	412	38	102	36336	356
16	100	36365	365	39	103	39614	385
20	87	32363	371	40	106	36627	345
Average		$R_s : 100$		$R_{sh} : 35292$		$R_{sh}/R_s : 356$	

Table S7 The values of R_{sh} , R_s and R_{sh}/R_s extracted from the J-V measurement of Annealing-PSCs from 40 devices.

Annealing-PSCs							
	R_s	R_{sh}	R_{sh}/R_s		R_s	R_{sh}	R_{sh}/R_s
1	125	37667	301	21	99	28473	289
2	127	35279	278	22	124	33021	266
3	161	50138	312	23	100	27929	278
4	97	28144	290	24	156	46793	300
5	112	34572	308	25	102	32551	318
6	109	38945	356	26	135	39985	296
7	101	29870	297	27	124	34533	278
8	152	46884	308	28	100	22962	230
9	74	23533	318	29	118	28279	240
10	140	47588	341	30	120	34096	283
11	80	25958	324	31	110	28102	256
12	98	31127	318	32	115	29573	257
13	98	26321	268	33	103	23777	231
14	120	34326	286	34	113	28923	256
15	125	35174	281	35	133	42440	318
16	122	29359	240	36	140	33633	241
17	127	34037	269	37	115	28511	248
18	132	34639	263	38	114	2631	230
16	101	23282	230	39	118	28279	240
20	112	25931	231	40	99	22841	231
Average		$R_s : 116$		$R_{sh} : 31753$		$R_{sh}/R_s : 278$	

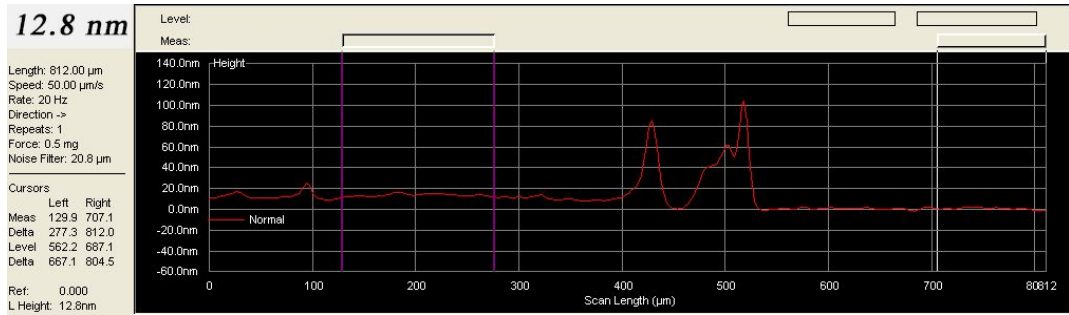


Fig. S1 Spectrum for the thickness measurement of ZrO_2 film.

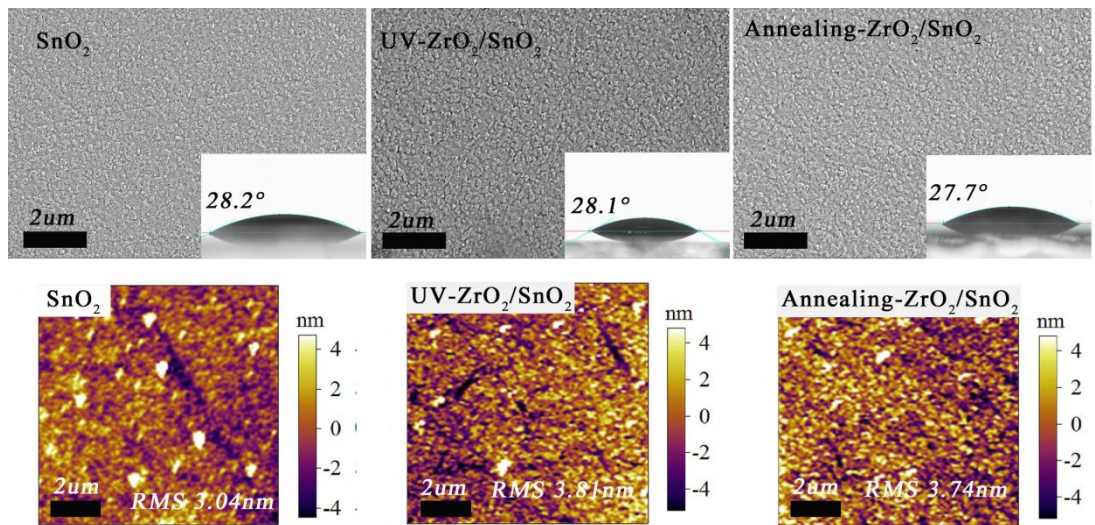


Fig. S2 The top-view SEM images and the water contact angle image (a) SnO_2 , (b) UV- $\text{ZrO}_2/\text{SnO}_2$ and (c) Annealing- $\text{ZrO}_2/\text{SnO}_2$. AFM images ($10 \times 10 \mu\text{m}$) of (d) SnO_2 , (e) UV- $\text{ZrO}_2/\text{SnO}_2$ and (f) Annealing- $\text{ZrO}_2/\text{SnO}_2$ films, respectively.

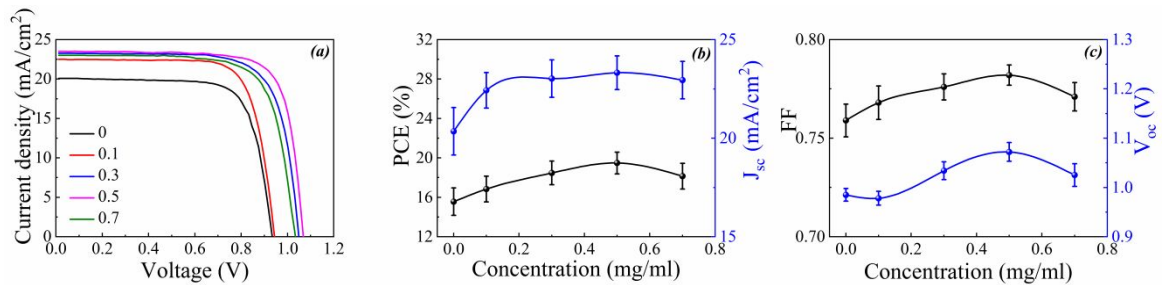


Fig. S3 (a) J-V curves of UV-PSCs with different precursor concentrations. (b) and (c) PCE, J_{sc} , FF and V_{oc} as functions of concentrations.

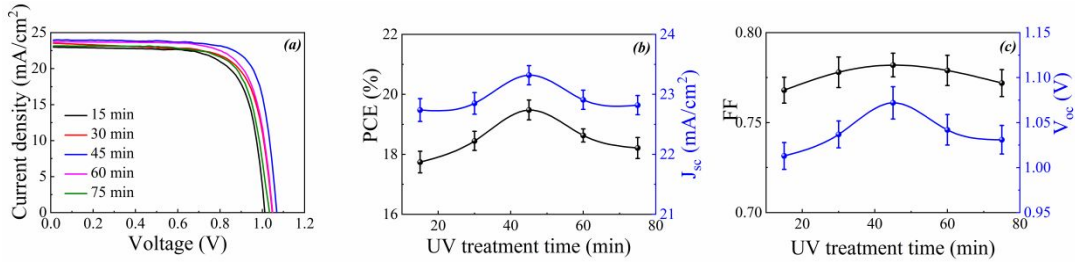


Fig. S4 (a) J-V curves of UV-PSCs with different UV treatment time. (b) and (c) PCE, J_{sc}, FF and V_{oc} as functions of time.

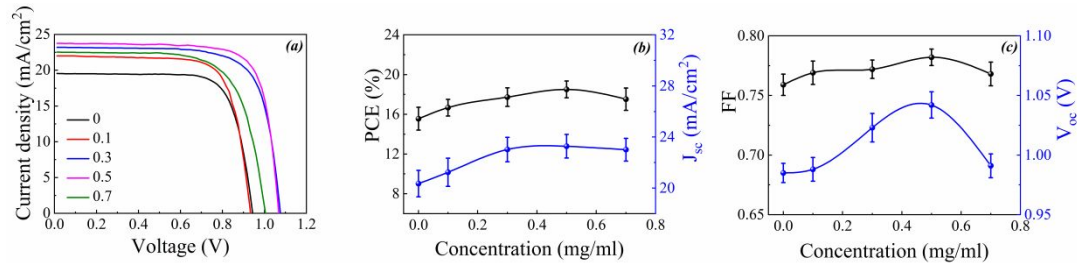


Fig. S5 (a) J-V curves of Annealing-PSCs with different precursor concentrations. (b) and (c) PCE, J_{sc}, FF and V_{oc} as functions of concentrations.

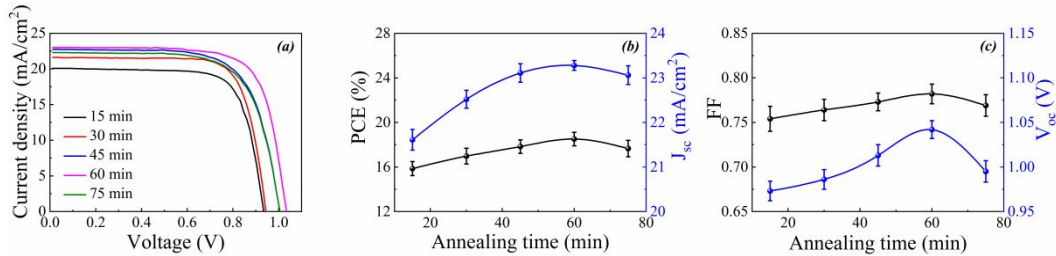


Fig. S6 (a) J-V curves of Annealing-PSCs with different annealing time. (b) and (c) PEC, J_{sc}, FF and V_{oc} as functions of time.

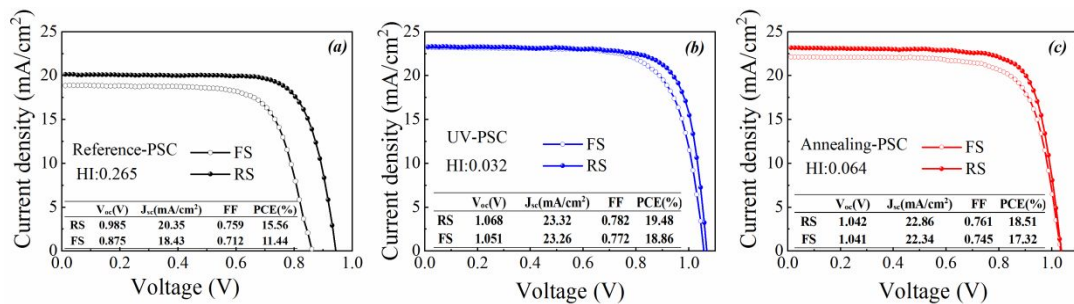


Fig. S7 J-V curves of the best-performing devices measured in both the reverse and forward scan directions: (a) Reference-PSC, (b) UV-PSC and (c) Annealing-PSC.

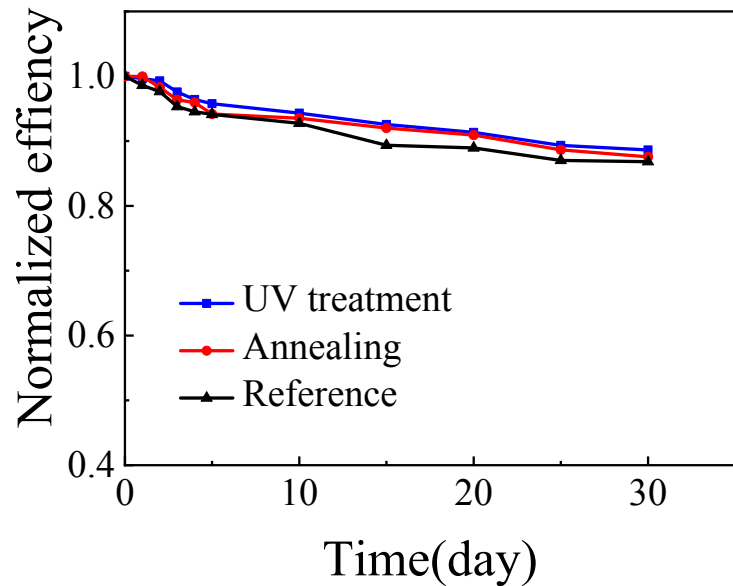


Fig. S8 Normalized PCE of unsealed Reference-, UV- and Annealing-PSCs stored in air.

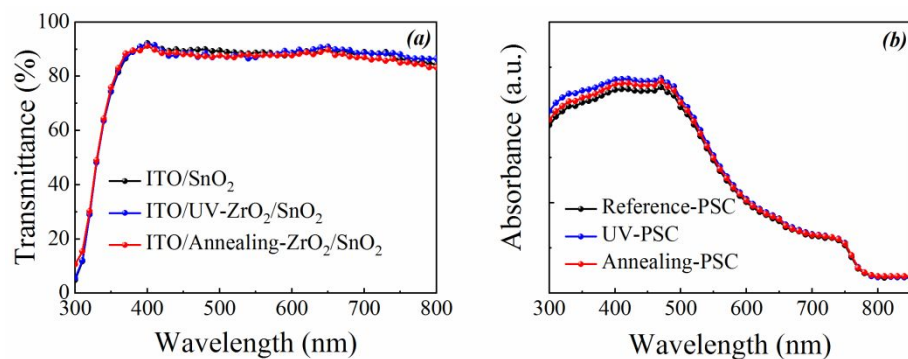


Fig. S9 (a) Transmittance spectra of ITO/SnO₂, ITO/UV-ZrO₂/SnO₂ and ITO/A annealing-ZrO₂/SnO₂. (c) Absorption spectra of Reference-PSC, UV-PSC and Annealing-PSC, respectively.

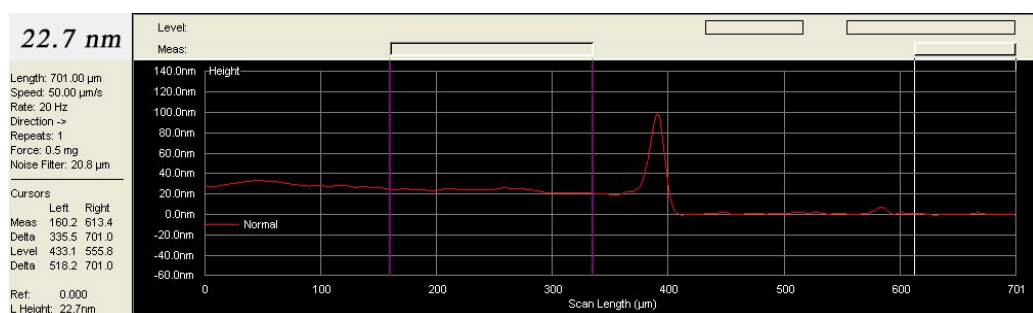


Fig. S10 Spectrum for the thickness measurement of SnO₂ film.

References

1. Liu, H.; Zhang, Z. B.; Zhang, X.; Cai, Y. Y.; Zhou, Y.; Qin, Q. Q.; Lu, X. B.; Gao, X. S.; Shui, L. L.; Wu, S. J.; Liu, J. M., Enhanced performance of planar perovskite solar cells using low-temperature processed Ga-doped TiO₂ compact film as efficient electron-transport layer. *Electrochim. Acta* **2018**, 272, 68-76.
2. Zhou, Y.; Zhang, Z. B.; Cai, Y. Y.; Liu, H.; Qin, Q. Q.; Tai, Q. D.; Lu, X. B.; Gao, X. S.; Shui, L. L.; Wu, S. J.; Liu, J. M., High performance planar perovskite solar cells based on CH₃NH₃PbI_{3-x}(SCN)_x perovskite film and SnO₂ electron transport layer prepared in ambient air with 70% humidity. *Electrochim. Acta* **2018**, 260, 468-476.
3. Wang, J.; Wang, N.; Jin, Y.; Si, J.; Tan, Z.-K.; Du, H.; Cheng, L.; Dai, X.; Bai, S.; He, H.; Ye, Z.; Lai, M. L.; Friend, R. H.; Huang, W., Interfacial Control Toward Efficient and Low-Voltage Perovskite Light-Emitting Diodes. *Adv. Mater.* **2015**, 27 (14), 2311-2316.
4. Jeong, S.; Moon, J., Low-temperature, solution-processed metal oxide thin film transistors. *J. Mater. Chem.* **2012**, 22 (4), 1243-1250.
5. He, W.; Xu, W.; Peng, Q.; Liu, C.; Zhou, G.; Wu, S.; Zeng, M.; Zhang, Z.; Gao, J.; Gao, X.; Lu, X.; Liu, J. M., Surface Modification on Solution Processable ZrO₂ High-k Dielectrics for Low Voltage Operations of Organic Thin Film Transistors. *J. Phys. Chem. C* **2016**, 120 (18), 9949-9957.